Philosophical Magazine

ISSN: 1478-6435 (Print) 1478-6443 (Online) Journal homepage: http://www.tandfonline.com/loi/tphm20

Stored energy in metallic glasses due to strains within the elastic limit

A. L. Greer & Y. H. Sun

To cite this article: A. L. Greer & Y. H. Sun (2016) Stored energy in metallic glasses due to strains within the elastic limit, Philosophical Magazine, 96:16, 1643-1663, DOI: 10.1080/14786435.2016.1177231

To link to this article: http://dx.doi.org/10.1080/14786435.2016.1177231

Published online: 02 May 2016.

PHILOSOPHICAL MAGAZINE, 2016
VOL. 96, NO. 16, 1643–1663
http://dx.doi.org/10.1080/14786435.2016.1177231

Taylor & Francis
Taylor & Francis Group

Stored energy in metallic glasses due to strains within the elastic limit

A. L. Greer[a,b] and Y. H. Sun[a]

[a]Department of Materials Science & Metallurgy, University of Cambridge, Cambridge, UK; [b]WPI Advanced Institute for Materials Research, Tohoku University, Sendai, Japan

ABSTRACT

Room temperature loading of metallic glasses, at stresses below the macroscopic yield stress, raises their enthalpy and causes creep. Thermal cycling of metallic glasses between room temperature and 77 K also raises their enthalpy. In both cases, the enthalpy increases are comparable to those induced by heavy plastic deformation, but, as we show, the origins must be quite different. For plastic deformation, the enthalpy increase is a fraction (<10%) of the work done (WD) (and, in this sense, the behaviour is similar to that of conventional polycrystalline metals and alloys). In contrast, the room temperature creep and the thermal cycling involve small strains well within the elastic limit; in these cases, the enthalpy increase in the glass exceeds the WD, by as much as three orders of magnitude. We argue that the increased enthalpy can arise only from an endothermic disordering process drawing heat from the surroundings. We examine the mechanisms of this process. The increased enthalpy ('stored energy') is a measure of rejuvenation and appears as an exothermic heat of relaxation on heating the glass. The profile of this heat release (the 'relaxation spectrum') is analysed for several metallic glasses subjected to various treatments. Thus, the effects of the small-strain processing (creep and thermal cycling) can be better understood, and we can explore the potential for improving properties, in particular the plasticity, of metallic glasses. Metallic glasses can exhibit a wide range of enthalpy at a given temperature, and small-strain processing may assist in accessing this for practical purposes.

ARTICLE HISTORY
Received 7 January 2016
Accepted 4 April 2016

KEYWORDS
Metallic glasses; calorimetry; creep; deformation mechanisms; glass transition

1. Introduction

Metallic glasses have exceptionally high yield stresses, and their elastic strain limit under uniaxial loading is ~2%, much larger than for conventional engineering alloys. Plastic deformation is accompanied by dilatation and softening, and this leads to flow being sharply localized into *shear bands* [1]. In uniaxial tension, shear band formation leads to catastrophic failure such that the ductility (plasticity in *tension*) is effectively zero. Yet metallic glasses can

CONTACT A. L. Greer alg13@cam.ac.uk
All data accompanying this publication are directly available within the publication.

show considerable plasticity in *compression* and in bending, and their fracture toughness can be as high as 232 MPa $m^{1/2}$ [2].

An as-cast glass when annealed undergoes structural relaxation into states of lower energy and higher density, generally with worsened mechanical properties: increased localization of strain (fewer shear bands with larger offset on each), leading to reduced plasticity in compression and bending. Ultimately, the glasses can become fully brittle, with fracture toughness similar to oxide glasses.

Given these effects of relaxation (*ageing*), there is clear interest in structural evolution in the opposite direction, towards states of higher energy and lower density. Such *rejuvenation* can be achieved by purely thermal means, by heating the glass into the liquid state and then cooling sufficiently rapidly back into the glassy state [3]. While it has been suggested that this could be applied to as-cast metallic-glass components [3], there is a risk of shape change through viscous flow above the glass-transition temperature, T_g, and it would be impossible to achieve sufficient cooling rate throughout larger components.

Staying within the solid glassy state, rejuvenation has also been achieved by plastic deformation [4–8] and by ion and neutron irradiation [9,10]. Such processes inject energy into the glass and some fraction of that is stored in higher-energy structural states. The treated materials show significantly improved mechanical properties [9,11–16]. There are even indications that sufficiently rejuvenated glasses can show ductility; this may arise because flow in a glass of low density may facilitate densification rather than the usual dilatation [17]. But mechanical deformation cannot be readily applied to already shaped components, and neutron irradiation has problems of limited access to treatment facilities, and transmutation, particularly to radioactive nuclides. While ion irradiation can rejuvenate nanoscale samples, the limited depth of primary knock-on damage (e.g. ~20 nm for 30 kV Ga^+ ions [9]), prevents effective treatment of larger samples.

In 2008, Lee et al. [18] reported that compressive loading of a $Cu_{65}Zr_{35}$ (compositions are given in at.% throughout) glass in the *elastic* range led to rejuvenation and to improvements in mechanical properties. This elastostatic loading was at room temperature (~0.4 T_g), at 90% of the macroscopic yield stress σ_y, for 12 h. Subsequent mechanical tests in compression showed that the plastic strain at failure had increased from effectively zero to 5.2% as a result of this treatment. There has been much further work confirming such effects [19–24], including direct verification that the density of samples decreases as a result of the loading [25]. The density decreases, despite the compressive loading, because the shear component of the applied stress leads to creep and this uniform time-dependent flow induces dilatation.

Recently, it has been shown that thermal cycling of metallic-glass samples between room temperature and liquid-nitrogen temperature (77 K) can also induce significant rejuvenation and improvement of mechanical properties [26,27]. As a method for rejuvenation, thermal cycling is particularly attractive. It is non-destructive, isotropic, inducing no shape change, applicable to any sample geometry (thin film, ribbon, bulk, shaped component), affecting the whole sample (not just the surface as, e.g. in shot-peening [28] or ion irradiation [9], and not just in or near shear bands), and repeatable as necessary.

The rejuvenation effects of elastostatic loading and of thermal cycling are the focus of this paper. While the practical interest may centre on improvement of mechanical properties, the stored energy induced by these treatments is the most straightforward quantitative guide to the degree of rejuvenation. Very surprisingly, these apparently mild treatments (in which strains are always well within the elastic limit) give stored energies similar to those resulting from severe plastic deformation. We examine the possible origins of the stored energy and

show that these must be different from those that operate in energetic processing (plastic deformation and irradiation). Understanding the mechanisms may permit new extremes of the glassy state in metals to be reached, with the prospect that highly rejuvenated states could have properties of fundamental and practical interest.

2. Values of stored energy

2.1. Cold work in polycrystals

To provide background, we consider first the understanding of stored energy induced by cold work (i.e. deformation below the recrystallization temperature, usually at room temperature) of conventional polycrystalline metals and alloys. This subject has been comprehensively reviewed by Bever et al. [29]. In the early stages of room temperature deformation (by such processes as rolling and wire drawing) less than 10% of the mechanical WD on a sample is stored in the material, the rest being dissipated as heat. The deformation induces damage, increasing the population of defects (dislocations, vacancies, stacking faults, twins) and changes the distribution of grain boundaries and phases. As deformation continues to higher strain, the induced damage, specifically the concentrations of defects such as dislocations, must eventually saturate. A steady state is reached in which the rate of damage is balanced by the rate of repair through annealing processes that may themselves be accelerated by the increased defect densities. The steady state corresponds to a higher level of damage (i.e. the material has a higher stored energy) if the strain rate is higher or the temperature is lower, reflecting the balance of the damage and repair rates [30]. Stored energies in materials of different compositions are best compared as molar quantities. These can be considered relative to the latent heat of melting ΔH_m, an energy representing destruction of the crystal structure.

For conventional working of polycrystalline pure metals, the maximum stored energy is a few 100 J g-atom^{-1} (1–2% of ΔH_m) and for solid solutions this increases to nearly 1 kJ g-atom^{-1} (5–10% of ΔH_m) [29]. Obviously, as its saturation value is approached, the stored energy constitutes a diminishing fraction of the mechanical WD.

2.2. Stored energy in as-cast glasses

It is important to note that, unlike crystalline alloys, metallic glasses can show significant stored energies, even without any deformation. As for glasses in general, the state of an as-cast metallic glass depends on the cooling rate at which it was formed. In a typical differential scanning calorimetry (DSC) run, the heating rate is of the order of 20 K min^{-1}, and this is lower than the rate at which the glass was formed. Consequently, before the glass transition is reached on heating, the glass relaxes towards lower-energy states characteristic of slower cooling. This relaxation is manifest as an exothermic peak in the DSC trace. After heating above T_g, the sample is cooled at the same rate as the initial heating, and a second heating run, now on the relaxed glass, again at the same rate, is used to obtain a baseline. The relaxation during the first heating run is then characterized as the difference between the first and second heating traces [28,31]. Alternatively, the first heating run can be taken to a temperature high enough to crystallize the glass; the crystalline state then sets the baseline in the second run [24,32]. Integration of the area between the two heating traces gives the total heat of relaxation ΔH_{rel}. This can be compared with ΔH_m, which for

metallic-glass-forming compositions is 5–12 kJ g-atom^{-1}; we take 9 kJ g-atom^{-1} as representative of metallic glasses in general.

In as-cast metallic glasses, the heat release associated with structural relaxation is spread over a wide temperature range up to T_g. The form of this exotherm will be considered in §3; for the moment we focus only on the total heat ΔH_{rel}. As expected, ΔH_{rel} is higher for glasses cooled at higher rate, and values as high as 5.5 kJ g-atom^{-1} have been reported for melt-spun ribbons that are only 20 μm thick [31]. More usual values are 1–1.5 kJ g-atom^{-1} (11–17% of ΔH_m) for melt-spun ribbons and ~300 J g-atom^{-1} (~3% of ΔH_m) for bulk metallic glasses (BMGs) [6,7,28], that are, of course, more slowly cooled.

Figure 1 is schematic, but based closely on the BMG system $Zr_{52.5}Cu_{17.9}Ni_{14.6}Al_{10}Ti_5$. The temperature-dependent relative enthalpies, $H(T)$, are shown for the crystalline and liquid (equilibrium and supercooled) states, based on measured data [33]. The enthalpies of the glassy state are higher than that of the crystalline state, but are taken to have the same temperature dependence. The glass transition occurs at a liquid viscosity that is inversely proportional to the cooling rate, scaling relative to a viscosity of 10^{12} Pa s on cooling at 20 K min^{-1} (0.33 K s^{-1}); the glass-transition temperatures at other cooling rates are based on a temperature dependence of liquid viscosity ('fragility') between those of Zr-based and Pd-based BMGs [34]. Effective cooling rates range up to 10^{13} K s^{-1}, and higher, achieved in electrical pulse heating [35] and estimated in molecular-dynamics simulations of irradiation [10]. At such high rates, $T_g > T_m$. At the other extreme, ultrastable glasses achieved by thin-film deposition have such low enthalpies that the effective cooling rate is impractically low, of the order of 10^{-14} K s^{-1} [30,36]. With such a range, the glassy state has a spread of

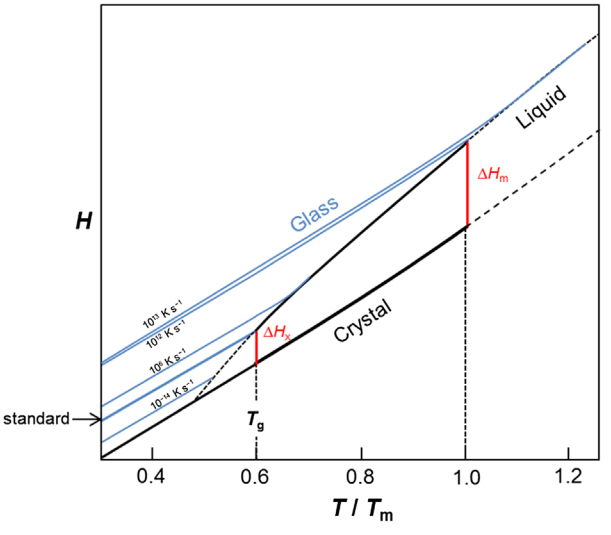

Figure 1. (colour online) Relative enthalpy versus reduced temperature for a typical bulk-metallic-glass-forming system. For such systems: the heat of melting ΔH_m is in the range 5–12 kJ g-atom^{-1} and we can take 9 kJ g-atom^{-1} as representative; the glass-transition temperature and the melting temperature (more strictly the liquidus temperature) are related by $T_g \approx 0.6\, T_m$; and at T_g, the heat of crystallization $\Delta H_x \approx 0.4\, \Delta H_m$. The plot is based on the measured enthalpies for the BMG $Zr_{52.5}Cu_{17.9}Ni_{14.6}Al_{10}Ti_5$ [33] and shows the values of ΔH and specific heat (dH/dT) correctly scaled. The glass transition is conventionally taken to occur at a liquid viscosity of 10^{12} Pa s on cooling at 0.33 K s^{-1}. Values of T_g at other cooling rates are obtained by scaling according to a temperature dependence of viscosity between those of Zr-based and Pd-based BMGs [34].

enthalpy that is >0.9 ΔH_m. That the range of enthalpy within the glassy state can be so large provides a motivation for the present study.

It is evident in Figure 1 that as the liquid is supercooled from T_m down to T_g, its enthalpy decreases faster than that of the crystalline state. This corresponds to the liquid having a higher specific heat capacity C_p. Integrating over (C_p/T) gives the changes in entropy on cooling, and these have a form similar to that for enthalpy in Figure 1 [33]; the entropy of the liquid exceeds that of the crystal by ΔS_m at T_m, and this entropy difference decreases on supercooling. At the conventional T_g, the entropy of the supercooled liquid exceeds that of the crystal by only ~0.15 ΔS_m. Quenching at different rates can freeze into the glass a range of entropy that is (relative to the equilibrium difference between liquid and crystal at T_m) just as wide as (perhaps even wider than) the range in enthalpy. Viewed in terms of entropy, faster-cooled glasses are more disordered; relaxation and rejuvenation treatments lead, respectively, to ordering and disordering. For quantification of the differences in glassy states, however, we continue to use enthalpy rather than entropy.

The range of glassy-state enthalpies accessible by thermomechanical processing has been reviewed elsewhere [30]. For the ease of comparison, we outline key results in §2.3, which provides a background for the new analyses in §2.4 and §2.5.

2.3. Stored energy from plastic deformation

The stored energy of cold work in metallic glasses was first studied by Chen [4], who rolled a pre-relaxed ribbon of $Pd_{77.5}Cu_6Si_{16.5}$ glass to a reduction in thickness of 34%. In this range of strain, the stored energy rose linearly with strain and constituted ~4% of the WD. Deformation to higher strains, for example to a 60% reduction in thickness in cold-rolling [6], or to much greater strains in high-pressure torsion [7], shows that the increase in ΔH_{rel} tends towards saturation. Thus, in terms of the fraction of WD that is stored during initial deformation, and of the tendency to establish a steady state at high strain, the behaviour of metallic glasses closely resembles that of polycrystalline metals and alloys. Heavily cold-rolled metallic glasses, with a reduction in thickness of 50–60%, show a stored energy of cold work of 300–450 J g-atom^{-1} (3–5% of ΔH_m) [4–6,8].

When as-cast metallic glasses are deformed, ΔH_{rel} can decrease, as observed for a Zr-based BMG subjected to spherical indentation [37] and a Pd-based BMG subjected to shot peening [28]. The as-cast glasses are in a higher energy state than can be achieved even by heavy plastic deformation. In the latter case, when the glass is pre-annealed, shot peening does lead to an increase in its ΔH_{rel} [28]. The peening-induced rejuvenation of the annealed glass is a stronger effect when the peening is conducted at 77 K than at room temperature, just as expected from the discussion of damage and repair rates in §2.1. In a Zr-based BMG cold-rolled to thickness reductions of up to 50%, ΔH_{rel} first increases and then decreases, matching well with changes in free volume indicated by positron-annihilation lifetime spectroscopy (PALS) [38].

2.4. Stored energy from elastostatic loading

Uniaxial compression at constant load (well within the elastic range) has been applied for several hours to bulk metallic glass rods at room temperature [18–24]. On application of the load, the sample shows an instantaneous elastic strain ε_e, then, with continued loading

time, a time-dependent anelastic strain ε_a that saturates, and finally a linearly increasing viscoplastic strain ε_v. On unloading, ε_e instantaneously recovers, then ε_a recovers over a time similar to that over which it developed. The sample is left with a permanent strain (i.e. it is shorter than initially) representing the value of ε_v at the point of unloading. For $Ni_{62}Nb_{38}$ (T_g = 913 K) and for $Cu_{65}Zr_{35}$ (T_g = 753 K), room temperature (298 K) is 0.33–0.40 T_g; in these cases ε_a develops, and recovers, fully within a few hours [18,19]. All the measurements of the effects of such 'elastostatic' loading are made after the anelastic recovery is complete.

After elastostatic loading, the samples show an increase in ΔH_{rel}. Studies of the effect of loading time show clearly that the increase is associated only with the viscoplastic strain component ε_v [21,22]. After an initial period of slow increase, in which ε_a is the dominant component of the strain, there is a sharp increase in ΔH_{rel} followed by saturation at longer loading times. Some final, near-saturation, levels of stored energy are collected in Table 1. These are the amounts by which the heat of relaxation has increased over that of the as-cast glass. Comparison of rows 2 and 5 in the Table suggests that, in steady state, the creep-induced increase in ΔH_{rel} is roughly proportional to the applied stress.

Elastostatic loading permits straightforward calculation of the WD. As ε_e and ε_a are fully recovered, the WD by the loading system, per unit volume of the sample, is simply the product of the applied stress and the final value of ε_v. Where these can be estimated from the original publications, the values of WD are also given in Table 1. In calculating the various gramme-atomic quantities, use was made of the values in Table A1 (in Appendix 1).

The energy values in Table 1 lead to a number of observations. First, it is notable that elastostatic loading can give stored energies of 247 J g-atom^{-1}, nearly as high as those after heavy cold-rolling (§2.3). It is remarkable that such an apparently gentle treatment as loading in the elastic regime can have such a large effect. Second, comparing the data in rows 9 and 10 of Table 1, the stored energy is significantly higher on loading at 77 K than at room temperature; we can conclude that the damage relaxation (repair) rate at room temperature is not negligible [24].

It is immediately evident that the stored energy exceeds the mechanical WD. The concept, well known from plastic deformation, that the stored energy is a fraction (usually a small fraction) of the WD (§2.1 and §2.3), is not supportable. This is seen even more clearly in the early stages of loading, well before the steady state is attained. For example, comparing

Table 1. Compressive elastostatic loading of metallic glasses. Application of stress at a given temperature causes an increase in the heat of relaxation ΔH_{rel}. The values given here are for the longest loading times and represent conditions near to steady state (i.e. saturated values of ΔH_{rel}). Where viscoplastic strains ε_v (always < 0.4%) are clear from the original publications, they have been used to calculate the mechanical WD. The ratio ΔH_{rel}/WD > 1, showing that the conventional concept of stored energy as a fraction of plastic WD cannot apply [18–22,24].

	Glass composition (at.%)	Stress (GPa)	$\frac{\text{Stress}}{\sigma_y}$	Time (h)	Temp.	ΔH_{rel} (J g-atom^{-1})	WD (J g-atom^{-1})	$\frac{\Delta H_{rel}}{WD}$	Ref.
1	$Cu_{65}Zr_{35}$	2.07	0.90	12	RT	133	52.1	2.55	[18]
2	$Cu_{65}Zr_{35}$	2.07	0.90	24	RT	194	34.25	5.66	[20]
3	$Ni_{62}Nb_{38}$	3.0	0.95	30	RT	179	95.9	1.87	[19]
4	$Cu_{50}Zr_{50}$	1.44	0.90	24	RT	49.5	6.68	7.41	[21]
5	$Cu_{65}Zr_{35}$	1.44	0.63	24	RT	116	6.24	18.6	[21]
6	$Cu_{50}Zr_{50}$	1.44	0.90	12	RT	43.3	5.77	7.50	[22]
7	$Cu_{57}Zr_{43}$	1.80	0.90	12	RT	127	20.19	6.28	[22]
8	$Cu_{65}Zr_{35}$	2.07	0.90	12	RT	174	35.41	4.92	[22]
9	$Cu_{57}Zr_{43}$	1.7	0.85	24	RT	132	–	–	[24]
10	$Cu_{57}Zr_{43}$	1.7	0.85	24	77 K	247	–	–	[24]

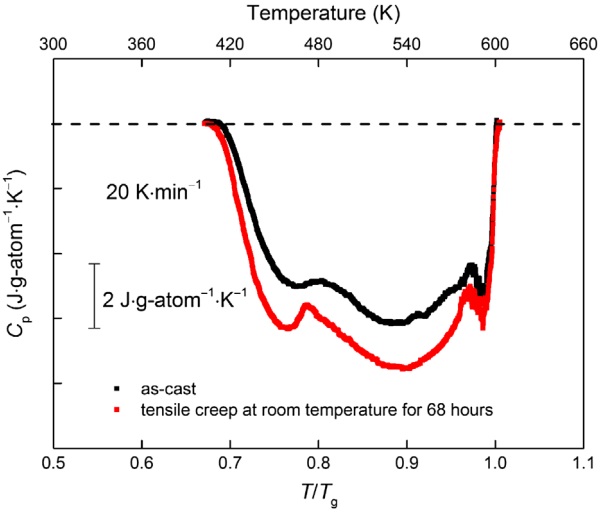

Figure 2. (colour online) DSC signals (the difference between first and second heating runs at 20 K min^{-1}) for an as-cast sample of $Pd_{40}Cu_{30}Ni_{10}P_{20}$ BMG and for a sample subjected to tension at 1% of the yield stress at room temperature for 68 h. In such a plot, exothermic processes give a downward deflection, and the area below the baseline (dashed) represents the total heat of relaxation (ΔH_{rel}). The tensile loading induces creep and leads to an increase of ΔH_{rel} from 605 to 763 J g-atom^{-1}. The temperature scale is plotted relative to T_g to facilitate comparison with Figures 3 to 5.

with row 5 in Table 1 for the same glass and loading conditions, the earliest point at which ΔH_{rel} and WD can be evaluated is after ~6 h of loading [21], by which point the strain is dominated by the viscoplastic component ε_v. At this point, the increase in heat of relaxation ΔH_{rel} = 85.7 J g-atom^{-1}, while WD = 1.56 J g-atom^{-1}, giving a ratio of ΔH_{rel}/WD = 55. In these early stages of loading, the stored energy is very much higher than the WD. The origin of the stored energy is considered in §4.

The work so far on elastostatic loading has applied compression to BMG samples. We have made a test of the effect of tension, applied to a 40-μm-thick melt-spun ribbon of $Pd_{40}Cu_{30}Ni_{10}P_{20}$. A stress of 12 MPa, 1% of the yield stress σ_y = 1.2 GPa, was applied for 68 h at RT. Then, the sample was stored stress-free for five days at RT to allow the anelastic strain to relax to zero. Figure 2 compares the DSC trace obtained on heating the treated sample at 20 K min^{-1} with that for an as-cast sample. There is a clear increase in ΔH_{rel}, of 158 J g-atom^{-1}, comparable with the values in Table 1. It is remarkable that there can be such a large effect with such a low applied stress (and ε_v below our resolution limit). These preliminary results suggest that elastostatic loading in tension may be much more efficient than compression in inducing rejuvenation. Although the rejuvenation is driven by shear (giving the viscoplastic creep strain ε_v), it is possible that the hydrostatic component of the applied stress is relevant. If so, we would expect rejuvenation, which is associated with a reduction in density, to be favoured by hydrostatic tension.

2.5. Stored energy from thermal cycling

Ketov et al. [26] found that several metallic glasses show significant rejuvenation effects (including improved compressive plasticity, and reversal of annealing-induced

embrittlement) induced by cycling between room temperature and 77 K. This temperature range is below that normally associated with thermal relaxation processes, and the rejuvenation can have no link with that induced by cycling through T_g (§1 [3]). For La-based melt-spun ribbons and bulk glasses, the ΔH_{rel} of as-cast samples increases by ~50% after 10–15 cycles. Melt-spun ribbons of $La_{55}Ni_{20}Al_{25}$ glass show a maximum ΔH_{rel} increase of 340 J g-atom^{-1} after 10 cycles. This is substantially higher than the increases induced by elastostatic loading (§2.4, Table 1), and very much in the range associated with heavy plastic deformation (§2.3). That ΔH_{rel} first increases and then decreases as the treatment continues is similar to the behaviour reported by Flores et al. [38] for a Zr-based BMG subjected to cold-rolling (§2.3).

There were earlier reports [39–42] of the effects of cryogenic treatments (single holds for various times at 77 K). The reported effects include reduced yield stress and Young modulus [40]. Most of these studies were on ferromagnetic metallic glasses (melt-spun ribbons) and a variety of magnetic properties were found to change. The clearest results are for the Curie temperature T_C, which has been widely used to monitor the degree of relaxation. For glassy compositions, where annealing causes T_C to increase, a cryogenic hold causes T_C to decrease. For more rapidly quenched ribbons, the initial T_C is lower and shows a greater reduction as a result of the cryogenic hold. This behaviour is consistent with the cryogenic hold (which of course constitutes a single thermal cycle) giving rejuvenation and furthermore supports the idea that a more inhomogeneous (less relaxed) sample would be more susceptible to rejuvenation by thermal cycling.

Ketov et al. [26] have suggested that rejuvenation is associated with thermal cycling and not with ongoing change at 77 K. The measured effects on magnetic properties [39,40], however, show that a longer hold at 77 K can have a greater effect, and this merits study for cycling treatments.

Ketov et al. [26] attribute cycling-induced rejuvenation to a spatially inhomogeneous coefficient of thermal expansion (CTE) in the metallic glasses. As a result of this inhomogeneity, stresses develop, leading to elastic stored energy. This energy cannot be determined as easily as for elastostatic loading, but it can nevertheless be estimated. The spatial variation of bulk modulus in a metallic glass is taken to be of the order of ± 18% (standard deviation). The volumetric CTE, and therefore, the linear CTE would show a similar (but inverse) variation [26]. We estimate the linear CTE of the $La_{55}Ni_{20}Al_{25}$ melt-spun glass to be 1.3×10^{-5} K^{-1} (Appendix 1). Therefore, cooling from room temperature (298 K) to 77 K would correspond to a linear thermal contraction of 0.29%. We take the inhomogeneity in the glass and its CTE to lead to a root-mean-square (rms) elastic strain in the glass that is 18% of this thermal strain. Then, taking the elastic strain energy (per unit volume) to be $\frac{1}{2}E\varepsilon^2$, where E is the Young modulus (≈44 GPa [26]) and ε is the rms elastic strain, the elastic energy is 5.9 kJ m^{-3}. Given a gramme-atomic volume of 15.9 cm^3 g-atom^{-1} (Appendix 1), this energy is 94 mJ g-atom^{-1}. Making the extreme assumption that all of this 'elastic' energy ends up stored in the glass for each of the 20 stages (cooling and heating) in 10 cycles, the total stored energy would be 1.9 J g-atom^{-1}. In practice, only a small fraction of this energy would be expected to remain stored in the glass. Although the estimation of the possible elastic energy has been crude, it is clear that this energy from inhomogeneous thermal strain in the glass is far too small (by at least three orders of magnitude) to explain the measured increase in ΔH_{rel} (up to 340 J g-atom^{-1}) resulting from thermal cycling. Even more strongly than for elastostatic loading (§2.4, Table 1),

it is clear that mechanical WD cannot account for the increase in stored energy in the metallic glass.

3. The relaxation spectrum

On heating in DSC, ΔH_{rel} corresponds to a broad exotherm, the shape of which (the relaxation spectrum) was first considered by Chen and Coleman [43]. Some of the characteristic features (peaks) of the spectrum have temperatures very dependent on heating rate [24,43], reflecting a low activation energy according to the Kissinger analysis [44] (Figure 3); as far as possible, we try to make comparisons at a standard heating rate of 20 K min^{-1}. For as-cast metallic glasses, the spectrum starts at ~0.6 T_g and continues up to T_g itself [28,31,43]. Chen and Coleman [43] noted that the spectrum appears to include two broad relaxations. In their Pd-based melt-spun ribbons and bulk samples, the lower-temperature relaxation is a distinct shoulder on the low-temperature side (at 0.75–0.8 T_g) of the main peak near T_g. A similar spectrum is found for $Zr_{64}Cu_{16}Ni_{10}Al_{10}$ BMG [6]). In other cases, for example Fe- and Ni-based melt-spun ribbons [5,31], the spectrum appears monomodal with long approach to the main peak, or, in contrast, there is a quite separate low-temperature peak (e.g. at ~0.7 T_g for $Pd_{40}Cu_{30}Ni_{10}P_{20}$ BMG [28]) (Figure 3).

This diversity in behaviour is similar to that of the loss modulus seen on heating in dynamic mechanical analysis (DMA), where increasingly evident low-temperature relaxation has been classified as 'excess wing', 'broad hump' and 'peak' [45]. A Zr-based BMG similar in composition to that showing a shoulder in the DSC relaxation spectrum shows an 'excess wing' in DMA, and the Pd-based BMG showing a separate peak in DSC shows a 'broad hump' in DMA [6,28,45]. In both DSC and DMA, the peak near T_g can be taken to represent α-relaxation, that is, the set of processes corresponding to the formation of different glassy states near T_g. The DSC peak is variable for a given composition, an effect attributed to differences in cooling rate [5,28,43].

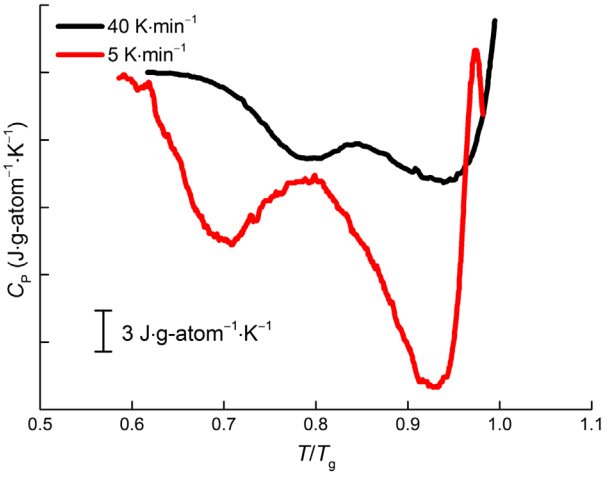

Figure 3. (colour online) The effects of heating rate on the relaxation spectrum: DSC signals for $Pd_{40}Cu_{30}Ni_{10}P_{20}$ BMG [28]. As the rate is increased from 5 to 40 K min^{-1}, the peaks in the relaxation spectrum shift to higher temperature, permitting determination of an effective activation energy by the Kissinger method [44].

The low-temperature processes represented by the shoulder or a separate peak can be taken to be β-relaxation, the principal dynamics in the glassy state [45,46]. Similarly as for the DMA results [45], it is probable that β-relaxation is always present in the DSC relaxation spectrum, but it may be so weak relative to α-relaxation that it appears only as a long low-temperature approach to, or shoulder on, the α-peak. From DMA studies, it is recognised that the activation energy of β-relaxation is the same as that for the operation of a shear transformation zone (STZ) and for the ductile-to-brittle transition [45]. When a metallic glass has a β-relaxation that is particularly easy to activate, it can show ductility in tension [47].

When a given composition is more rapidly quenched, both the α and β relaxations are more pronounced, with a stronger effect on the β relaxation [43]. For an as-cast BMG showing a bimodal relaxation spectrum in DSC, prior annealing preferentially removes the low-temperature β-relaxation peak, and it is restored after plastic deformation (shot peening), more effectively at 77 K than at room temperature [32] (Figure 4(a)); this is a particularly straightforward example of rejuvenation. Shot peening of an as-cast glass moves the start of the relaxation spectrum down to 0.55 T_g and the β-peak down to ~0.6 T_g [28] (Figure 4(b)). Where the relaxation spectrum of an as-cast glass is not bimodal, it can develop a low-temperature onset and a bimodal character after plastic deformation (cold-rolling) [5]. Shot peening of an as-cast Pd-based BMG caused a reduction in the α-peak, while leaving the β-peak largely unaffected [28,32]. Summarizing these observations, we can note that plastic deformation promotes the retention or growth of a β-peak in the DSC relaxation spectrum and moves the relaxation to lower temperatures relative to T_g. This further shows the link between the activation of STZs and β-relaxation.

The complexity of the relaxation spectrum after deformation is seen also in the free volume distribution revealed by PALS [38]. For a cold-rolled Zr-based BMG, it is suggested that there are three distinct size ranges for local volumes: (i) free volume in the dense glass, (ii) free volume in shear bands and other flow defects, and (iii) larger atomic-size voids [38]. Modifying an earlier discussion [32], we tentatively associate (i) with α-relaxation, (ii) with β-relaxation and (iii) with an extended low-temperature tail on the DSC relaxation spectrum. The energy in this low-temperature tail can decrease on holding at room temperature, an annealing effect that is especially evident in glasses with low T_g, giving a relaxation spectrum that starts at a higher fraction of T_g [48].

We next examine the effects of elastostatic loading and of thermal cycling on the relaxation spectrum. After elastostatic loading at room temperature, ΔH_{rel} is increased and begins to develop a low-temperature approach to [22], or shoulder on [24], the α-relaxation peak. For a $Cu_{57}Zr_{43}$ BMG (heated at 40 K min^{-1}), the start of the relaxation spectrum, at ~0.7 T_g in the as-cast glass, is displaced downwards to ~0.65 T_g after elastostatic loading; the α-peak also becomes stronger [24]. For the same glass, when the elastostatic loading is at 77 K, the effects are dramatic: although the onset is at the same temperature as for room-temperature loading, the relaxation becomes very clearly bimodal, with an α-peak much stronger than in the as-cast glass, and a new low-temperature peak of similar strength [24] (Figure 5(a)). The shift of the low-temperature peak with heating rate, according to the Kissinger analysis [44], gives an activation energy of 148 kJ g-$atom^{-1}$, in agreement with values obtained for the β-peak in DMA [24]. The activation energy of β-relaxation, as studied mainly by DMA, is found to be $26(\pm2)RT_g$ [45]. The activation energy for the low-temperature peak

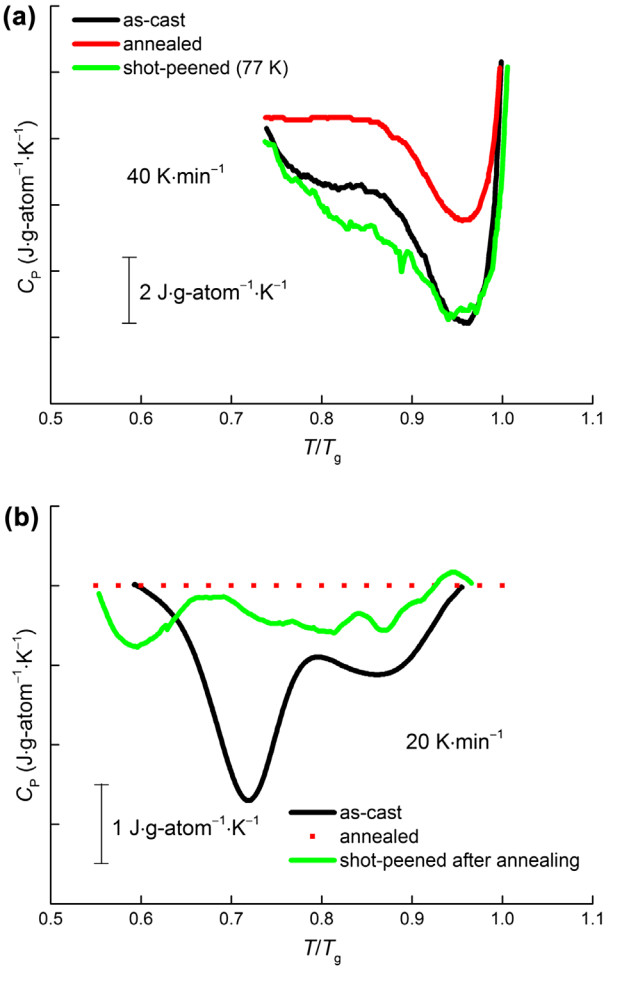

Figure 4. (colour online) Effects of annealing and plastic deformation on the relaxation spectrum: DSC signals for $Pd_{40}Cu_{30}Ni_{10}P_{20}$ BMG (heating at 20 K min^{-1}): (a) annealing (below or above T_g) removes the lower-temperature β-relaxation peak, and the peak is restored by shot peening (more effectively at 77 K than at RT) [32]; (b) shot peening of an as-cast glass moves the β-peak down to ~0.6 T_g [28].

in the DSC relaxation spectrum of $Cu_{57}Zr_{43}$ is $25RT_g$, consistent with this peak representing β-relaxation. At a heating rate of 20 K min^{-1}, this β-peak is at 583 K [24], which is ~0.8 T_g.

After thermal cycling of La-based metallic glasses (melt-spun ribbon and bulk), the initial broad featureless relaxation spectrum in DSC develops a clear bimodal character with the low-temperature peak (at ~0.9 T_g) stronger than the α-relaxation peak (also strengthened after cycling) nearer to T_g [26] (Figure 5(b)). Thermal cycling does not appear to have any effect on the onset temperature of the relaxation spectrum. This may, however, be because the onset of the spectrum is displaced to higher temperature by the room-temperature annealing effect [48] noted earlier for glasses with relatively low T_g.

From the relaxation spectra in DSC, it is clear that both elastostatic loading and thermal cycling can generate glassy states capable of greater low-temperature (presumed β)

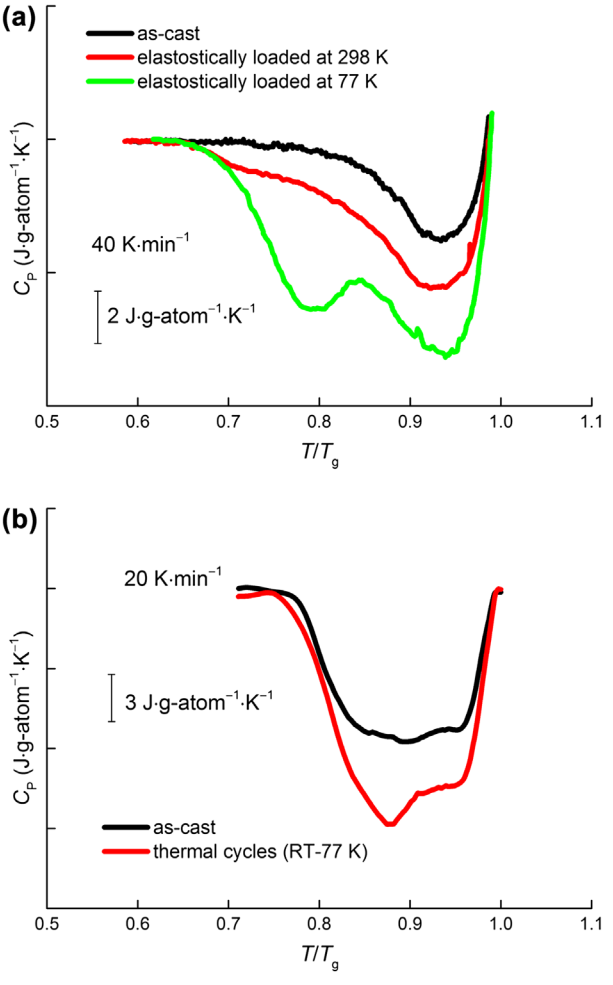

Figure 5. (colour online) Effects of small-strain treatments on the relaxation spectrum: DSC signals for: (a) $Cu_{57}Zr_{43}$ BMG showing that elastostatic loading, especially at 77 K, gives a new low-temperature peak [24]; (b) $La_{55}Ni_{20}Al_{25}$ melt-spun ribbon, showing that after 10 RT–77 K cycles the spectrum has a clear bimodal character [26].

relaxation. That these treatments also induce increases in plasticity [18,19,22,23,26] supports the suggested link [45] between β-relaxation and plasticity, even ductility.

We now compare the values noted earlier for the reduced temperatures (i.e. temperatures relative to T_g) for the β-peak or shoulder in the relaxation spectrum (at a common heating rate of 20 K min^{-1}). In as-cast glasses, the β-relaxation peak is at 0.7–0.8 T_g [6,28]; after plastic deformation, this is lowered to ~0.6 T_g [28]; after elastostatic loading at 77 K, this is at 0.8 T_g [24]; and after thermal cycling between room temperature and 77 K, this is at ~0.9 T_g [26]. Plastic deformation appears to generate sites activated at lower temperature, and treatments within the elastic regime (elastostatic loading and thermal cycling) to generate sites activated at higher temperature. In plastic deformation, however, the effects are inhomogeneous, with large effects expected within shear-bands, and smaller effects outside; in elastostatic and thermal straining, the effects are much more uniform.

4. Origins of stored energy induced by small strains

4.1. Endothermic disordering

We have seen that the increase in the enthalpy of metallic glasses subjected to elastostatic loading or thermal cycling cannot derive from mechanical work associated with the small strains in those treatments. The only possibility is that the increased enthalpy is associated with heat transfer from the surroundings. We suggest that elastostatic loading or thermal cycling induces a disordering process that is *endothermic*, drawing heat into the sample. Such a process would be analogous to melting of a system induced by raising the ambient temperature from marginally below to marginally above the melting point T_m. In such a case, as the temperature increase can be arbitrarily small, the energy associated with initially raising the temperature of an untransforming sample (analogous to the mechanical work in our current study) would be much smaller than the latent heat of melting ΔH_m. Rather, the system would melt progressively as the heat is drawn inward from the surroundings. Eventually, all of ΔH_m is supplied by the surroundings, and the system is fully melted. The now disordered system has a higher enthalpy and a higher entropy, but the associated free-energy decrease can be arbitrarily small. Parallels may also be found with shear-induced disordering and melting in colloidal systems [49,50].

Unlike melting, the disordering in the present case is not a sharp thermodynamically determined transition. Nevertheless, the picture of a progressive increase in entropy under essentially isothermal conditions can easily be applied to the effect of elastostatic loading, which has indeed been considered to induce structural disordering [20,22]. The nature of the disordering has been studied using molecular-dynamics (MD) simulations [20–22]. The structure of metallic glasses can be considered in terms of the polyhedral clusters of first-nearest neighbours around a central atom. The MD studies found that, under elastostatic loading, the proportion of densely packed (often icosahedral) clusters decreases, while the proportion of loosely packed clusters increases. Locally, the loading induces both the destruction and creation of densely packed clusters, but the former process predominates, especially when the clusters are isolated from others of similar high packing density [51]. A series of Cu–Zr compositions was the basis for systematic studies [21,22] of the effects of the packing density of as-cast metallic glasses. More densely packed glasses have higher yield stresses, lower plasticity, and lower ΔH_{rel}. As a result of elastostatic loading, more densely packed glasses show greater increases in plasticity and in ΔH_{rel}, such that the values for the different glasses tend to converge. MD simulations show that likewise the relative proportions of densely and loosely packed clusters in the different glasses tend to converge during elastostatic loading [21].

Remarkably, for three Cu–Zr glasses loaded at 90% of σ_y, it is the most densely packed, $Cu_{65}Zr_{35}$, that shows by far the largest viscoplastic strain ε_v [22,23]. Because σ_y for this glass is the highest of the three, it is loaded at the highest stress, but this effect is not nearly enough to account for the high ε_v. Rather, it seems that the accelerated creep is associated with the disordering itself; because this glass, in its as-cast state, is densely packed and relatively ordered, it has the greatest capacity for the generation of disorder [22]. The degree of disorder appears to reach a saturation level at long loading times; as noted in §2.4, this level (as judged from ΔH_{rel}) appears to depend on the applied stress.

As the studies of the effects of thermal cycling are still preliminary [26], a similar structural understanding of the observed increases in ΔH_{rel} has not yet emerged. Yet, based on the

similar evolutions of ΔH_{rel} and of the shape of the relaxation spectrum, it seems likely that the induced disorder must be similar. Although both elastostatic loading and thermal cycling set the conditions in which the disordering occurs, the process can be considered to be more spontaneous than driven, because the stored energy much exceeds the mechanical work.

For such disordering to proceed, heat must be drawn into the sample, and this requires the sample temperature to be below ambient. This slow disordering is thus in contrast to that in driven systems (e.g. those subjected to plastic deformation or irradiation) where the sample temperature rises above ambient because of the energy injected into the system. In analysing effects in the elastic range, it is of interest to consider the classical elastocaloric (also known as thermoelastic, piezocaloric, mechanocaloric) effect [29,52–54], linking thermal expansion and elasticity. We take the linear CTE to be positive as is the case for metallic glasses. In that case, a sample loaded adiabatically shows a temperature decrease when in tension and an increase in compression. Therefore, this temperature change is of the wrong sign to bring heat into metallic-glass samples under compressive elastostatic loading. Reiterating this point, under isothermal conditions (more directly relevant for elastostatic loading) uniaxial compression leads to a decrease in the entropy and a decrease in the heat content of the sample [29]. Indeed, ordering induced by elastic compression has been detected in a diffraction study of a Zr-based BMG [55]. There can be large elastocaloric effects near to a structural phase transition [54], but the signs of the adiabatic temperature change and isothermal entropy change remain the same. In any case, since the elastocaloric effect is reversible, essentially nondissipative, there should be no net change after loading and unloading.

The above discussion has emphasized effects in elastostatic loading. We turn now to thermal cycling and consider the flows of heat. As noted in §2.5, after 10 cycles from 298 K down to 77 K and back, $La_{55}Ni_{20}Al_{25}$ metallic-glass ribbons show an increase in ΔH_{rel} of 340 J g-atom^{-1}. Taking the specific heat of this metallic glass to be 25 J K^{-1} g-atom^{-1} (Appendix 1), the total heat flow out of (into) the sample in each cooling (heating) stage is 5.6 kJ g-atom^{-1}. For 10 cycles, the total flow, out and in, is 111 kJ g-atom^{-1}. The observed increase in ΔH_{rel} is 0.3% of this total. Put another way: in each cooling stage, the partial accumulation of stored energy means that 0.3% less energy is transferred to the liquid nitrogen than would otherwise be expected, that is, the effective C_p of the sample is lowered by 0.3%. Equivalently, in each heating stage, the effective C_p is increased by 0.3%. This 0.3% efficiency in converting thermal energy to structural damage in the material is only one tenth of the value (~4%) for the generation of damage by cold work of metallic glasses, but is still remarkably high. It seems that the thermal strains are rather efficient in disordering the sample (as are the early stages of viscous creep in elastostatic loading).

4.2. Mechanism of disordering

In plastic deformation, it is clear that the stresses involved are sufficient to generate defects. While in crystalline alloys the energies and entropies of the defects have been extensively characterized [29], the defects in metallic glasses are more difficult to define and characterize. In each case, however, the accumulation of defects can account for the associated stored energy of cold work. In contrast, in both elastostatic loading and thermal cycling, the strains are well below the elastic limit, and the challenge is to understand how these can lead to damage and disordering. We consider first elastic strains; the key points apply

for glasses in general, though of course our interest is in metallic glasses. As reviewed, for example, by Egami et al. [56], elastic strains must be *non-affine*. The non-uniformity of displacements resulting from elastic loading has been studied in atomistic simulations and in the changes in measured pair distribution functions induced by straining metallic-glass samples. It can be described in terms of a mechanical anisotropy emerging at small length-scales (<10–15 nm) [57].

The second key point is that, even for very low strains well within the elastic regime, there are local atomic rearrangements (shear transformations) that are not simply reversible: macroscopically the sample returns to its original dimensions, but individual atomic configurations are not exactly recovered. Egami et al. suggest that the strain at which the first shear events occur is $0.078/N$, where N is the number of atoms in the system [56]. Evidently, the strain is vanishingly small for real systems. Even in a small simulated system, local values of shear modulus G can extend to very low values, reflecting configurations that are near to instability [58]. Evidence for shear events at low strain comes from simulations [59], from viscoelastic measurements [60], and from the interpretation of the macroscopic values of elastic moduli of glasses [61]. The rearrangements contribute to elastic strains that are greater than would be seen otherwise (with affine displacements) and therefore give lower elastic moduli than in the crystalline counterpart materials.

Ketov et al. [26] suggested that in glasses, thermal strains should similarly be non-affine, and that they could therefore also lead to damage. There is direct evidence for non-affine thermal strains from diffraction studies [62]. The non-affine nature of elastic strains can be considered in terms of non-uniformity of the elastic moduli. The non-affine nature of thermal strains can be considered in terms of non-uniformity of the CTE. As moduli and CTE are closely related [26,63], similar effects can be expected from changing stress and changing temperature. A clear difference is that elastostatic loading is uniaxial, while thermal expansion/contraction is isotropic. The local strains arising from a temperature change, however, depend not only on the local CTE, but are influenced by the need to maintain elastic compatibility throughout the solid. In this way, local shear strains arise even though the macroscopic thermal strain is hydrostatic.

Ediger [64] suggests that the dynamics in glass-forming liquids are more heterogeneous for higher liquid fragility. Hence, we speculate that metallic glasses formed from more fragile liquids would be more susceptible to rejuvenation by thermal cycling. Greater initial heterogeneity in metallic glasses might also be achieved by phase separation, by partial crystallization, or by prior plastic deformation.

The present work focuses on quantification of the disordering through measurement of ΔH_{rel}, but it is also of interest to consider the associated reduction in density. For elastostatic loading, this was studied by Ke et al. [25]. A Zr-based BMG was subjected to uniaxial compression at 80% of σ_{y} for 50 h. After that treatment, the viscoplastic strain ε_{v} was -2.3×10^{-5} (misprinted as -2.3×10^{-4} in the original paper) and the fractional density change was -2.6×10^{-3}. That the density decrease is (relatively) so large invalidates the implicit 'constant-volume' assumption in [25]. Given the axial compressive strain ε_{v} and the overall volume expansion, we can derive that the sample expands laterally by a strain of 1.31×10^{-3} and that the effective shear strain is 6.7×10^{-4} in each of the axial-transverse planes. Argon [65] took the simple shear strain (ε_{12} when $\varepsilon_{21} = 0$) associated with operation (*flipping*) of an STZ to be of the order of 0.1, and the pure-shear ($\varepsilon_{12} = \varepsilon_{21}$) magnitude is thus 0.05. We avoid discussion of the typical size of STZs, but instead consider the volume

fraction F of the sample that they occupy. Thus a given effect could arise from a higher (or lower) population density of smaller (or larger) STZs. The macroscopic shear strain arises from the net number of STZs flipping in one direction rather than its reverse. If F is the volume fraction of this net number, then $F = \left(2 \times 6.7 \times 10^{-4} \big/ 0.05\right) = 2.68 \times 10^{-2}$.

The fractional increase in the volume of the sample (obtained from the measured density) is 2.6×10^{-3}. If we assume that under loading there are only positive STZ shears (each event is in the direction of, and directly driven by, the applied stress) then F would represent the total volume fraction of the STZs responsible for the measured strains. If we further assume that the volume increase of the sample occurs entirely within the STZs, then the volume of each STZ would have to increase by 10%. This is unreasonably large; judging from the dilatation frozen into shear bands [1,66], a more reasonable increase would be 1%. If we adopt the latter value, then the total volume fraction (and number) of activated STZs must be roughly 10 times the net. Therefore, it seems that the net number (positive minus negative) of STZs flipping in a given direction is at most 10% of the total number of flips. The large redundant fraction (positive flips cancelled by negative flips) is a measure of the degree of disordering induced by a very small uniaxial viscoplastic strain ε_v. This redundant fraction can be particularly associated with the endothermic disordering.

5. Conclusions

In the plastic deformation of conventional metals and alloys, it is well accepted that a fraction (typically <10%) of the WD is stored in the material in the form of increased defect densities. For metallic glasses, the mechanisms of deformation are quite different, and the defects are more difficult to characterize, but plastic deformation leads to a similar fraction of the WD being stored in the form of structural change. In the glasses, the increased enthalpy after deformation is a sign of rejuvenation, being opposite to the changes on relaxation or ageing. Irradiation is a further example of energetic processing in which a fraction of the energy injected into the sample is stored as structural change.

Recent work has shown that creep of metallic glasses at room temperature and below, induced by compressive loading at stresses well below the macroscopic yield stress ('elastostatic loading'), also leads to rejuvenation. But we find that the increases in enthalpy exceed the WD on the samples, by a factor of 50 or more in the early stages of loading. We present preliminary evidence that for tensile loading the increases in enthalpy are even higher relative to the WD, the component of hydrostatic tensile stress in the loading possibly aiding the reduction in density associated with rejuvenation.

Other recent work has shown that thermal cycling of metallic glasses between room temperature and liquid-nitrogen temperature (77 K) leads to even stronger rejuvenation, comparable with that seen after heavy plastic deformation. This effect is attributed to the action of internal stresses arising from non-uniformity of the CTE. In this case, we find that the increase in the enthalpy of the metallic glass is at least three orders of magnitude higher than any reasonable estimate of the internal WD.

The present work has focused on the enthalpy increases as a result of elastostatic loading and thermal cycling. In these processes, the strains are small, well within the elastic limit, yet structural changes are induced; the metallic glass behaves elastically at the macroscopic level but not completely so at the atomistic level. The increases in enthalpy cannot come from the energy induced by the processing methods themselves. We suggest that the energy

must come from the surroundings and that this happens because the processing induces an endothermic disordering process in the metallic-glass sample. This process involves non-affine strains at atomic level, and many redundant shear transformations. The disordering is accompanied by increases not only in enthalpy, but also in entropy and volume. It is of particular interest because it also leads to improved plasticity, specifically to less sharp localization of shear.

On heating metallic glasses, their excess enthalpy is annealed out over a range of temperature, the profile of the heat release being the 'relaxation spectrum'. The present work has the most comprehensive survey so far of relaxation spectra in glasses after various treatments. We identify three main elements in the heat release: (i) α relaxation near the glass-transition temperature T_g, associated with the different glassy structures that would be obtained on cooling at different rates; (ii) β relaxation at 0.7–0.9 T_g, associated with the excess ('free') volume in shear bands and other flow defects (and showing the same activation energy as for operation of an STZ); and (iii) relaxation at lower temperatures down to 0.55 T_g, associated with larger voids. Overall, the possible range of enthalpy in a metallic glass at a given temperature is wide, more than 90% of the heat of melting. Exploring a substantial fraction of that range by apparently benign and easily applied processes such as elastostatic loading and thermal cycling is of fundamental and practical interest, and the endothermic-disordering process by which this is achieved merits further study.

Disclosure statement

No potential conflict of interest was reported by the authors.

Funding

A. L. Greer was supported by the Engineering and the Engineering and Physical Sciences Research Council, UK [grant number EP/I035404/1]; the World Premier International Research Center Initiative (WPI), MEXT, Japan; Y. H. Sun. was supported by a China Scholarship Council (CSC) scholarship. All data accompanying this publication are directly available within the publication.

ORCID

A. L. Greer http://orcid.org/0000-0001-7360-5439

References

[1] A.L. Greer, Y.Q. Cheng, and E. Ma, *Shear bands in metallic glasses*, Mater. Sci. Eng. R 74 (2013), pp. 71–132.
[2] J. Xu and E. Ma, *Damage-tolerant Zr–Cu–Al-based bulk metallic glasses with record-breaking fracture toughness*, J. Mater. Res. 29 (2014), pp. 1489–1499.
[3] M. Wakeda, J. Saida, J. Li, and S. Ogata, *Controlled rejuvenation of amorphous metals with thermal processing*, Sci. Reports 5 (2015), Article ID 10545.
[4] H.S. Chen, *Stored energy in a cold-rolled metallic glass*, Appl. Phys. Lett. 29 (1976), pp. 328–330.
[5] B. Jessen and E. Woldt, *Stored energy of the deformed metallic glass $Ni_{78}Si_8B_{14}$*, Thermochim. Acta 151 (1989), pp. 179–186.
[6] J.W. Liu, Q.P. Cao, L.Y. Chen, X.D. Wang, and J.Z. Jiang, *Shear band evolution and hardness change in cold-rolled bulk metallic glasses*, Acta Mater. 58 (2010), pp. 4827–4840.

[7] F. Meng, K. Tsuchiya, S. Ii, and Y. Yokoyama, *Reversible transition of deformation mode by structural rejuvenation and relaxation in bulk metallic glass*, Appl. Phys. Lett. 101 (2012), Article ID 121914.
[8] O. Haruyama, K. Kisara, A. Yamashita, K. Kogure, Y. Yokoyama, and K. Sugiyama, *Characterization of free volume in cold-rolled $Zr_{55}Cu_{30}Ni_5Al_{10}$ bulk metallic glasses*, Acta Mater. 61 (2013), pp. 3224–3232.
[9] D.J. Magagnosc, G. Kumar, J. Schroers, P. Felfer, J.M. Cairney, and D.S. Gianola, *Effect of ion irradiation on tensile ductility, strength and fictive temperature in metallic glass nanowires*, Acta Mater. 74 (2014), pp. 165–182.
[10] R.E. Baumer and M.J. Demkowicz, *Radiation response of amorphous metal alloys: Subcascades, thermal spikes and super-quenched zones*, Acta Mater. 83 (2015), pp. 419–430.
[11] S. Takayama, *Drawing of $Pd_{77.5}Cu_6Si_{16.5}$ metallic glass wires*, Mater. Sci. Eng. 38 (1979), pp. 41–48.
[12] Y. Yokoyama, K. Yamano, K. Fukaura, H. Sunada, and A. Inoue, *Ductility improvement of Zr55Cu30Al10Ni5 bulk amorphous alloy*, Scripta Mater. 44 (2001), pp. 1529–1533.
[13] L. He, M.B. Zhong, Z.H. Han, Q. Zhao, F. Jiang, and J. Sun, *Orientation effect of pre-introduced shear bands in a bulk-metallic glass on its "work-ductilising"*, Mater. Sci. Eng. A 496 (2008), pp. 285–290.
[14] S. Scudino, B. Jerliu, K.B. Surreddi, U. Kühn, and J. Eckert, *Effect of cold rolling on compressive and tensile mechanical properties of $Zr_{52.5}Ti_5Cu_{18}Ni_{14.5}Al_{10}$ bulk metallic glass*, J. Alloys Comp. 509 (2011), pp. S128–S130.
[15] R. Gerling, F.P. Schimansky, and R. Wagner, *Restoration of the ductility of thermally embrittled amorphous alloys under neutron-irradiation*, Acta Metall. 35 (1987), pp. 1001–1006.
[16] R. Raghavan, K. Boopathy, R. Ghisleni, M.A. Pouchon, U. Ramamurty, and J. Michler, *Ion irradiation enhances the mechanical performance of metallic glasses*, Scripta Mater. 62 (2010), pp. 462–465.
[17] Y. Wang, W. Zhao, G. Li, Y. Li, and R. Liu, *Structural evolution of lanthanide-based metallic glasses under high pressure annealing*, J. Alloys Comp. 551 (2013), pp. 185–188.
[18] S.-J. Lee, B.-G. Yoo, J.-I. Jang, and J.-C. Lee, *Irreversible structural change induced by elastostatic stress imposed on an amorphous alloy and its influence on the mechanical properties*, Metal. Mater. Int. 14 (2008), pp. 9–13.
[19] S.-C. Lee, C.-M. Lee, J.-W. Yang, and J.-C. Lee, *Microstructural evolution of an elastostatically compressed amorphous alloy and its influence on the mechanical properties*, Scripta Mater. 58 (2008), pp. 591–594.
[20] S.-C. Lee, C.-M. Lee, J.-C. Lee, H.-J. Kim, Y. Shibutani, E. Fleury, and M.L. Falk, *Structural disordering process of an amorphous alloy driven by the elastostatic compression at room temperature*, Appl. Phys. Lett. 92 (2008), Article ID 151906.
[21] K.-W. Park, C.-M. Lee, M. Wakeda, Y. Shibutani, E. Fleury, and J.-C. Lee, *Homogeneous deformation of bulk amorphous alloys during elastostatic compression and its packing density dependence*, Scripta Mater. 59 (2008), pp. 710–713.
[22] K.-W. Park, C.-M. Lee, M. Wakeda, Y. Shibutani, M.L. Falk, and J.-C. Lee, *Elastostatically induced structural disordering in amorphous alloys*, Acta Mater. 56 (2008), pp. 5440–5450.
[23] K.-W. Park, C.-M. Lee, M.-R. Lee, E. Fleury, M.L. Falk, and J.-C. Lee, *Paradoxical phenomena between the homogeneous and inhomogeneous deformations of metallic glasses*, Appl. Phys. Lett. 94 (2009), Article ID 021907.
[24] J.-C. Lee, *Calorimetric study of β-relaxation in an amorphous alloy: an experimental technique for measuring the activation energy for shear transformation*, Intermetallics 44 (2014), pp. 116–120.
[25] H.B. Ke, P. Wen, H.L. Peng, W.H. Wang, and A.L. Greer, *Homogeneous deformation of metallic glass at room temperature reveals large dilatation*, Scripta Mater. 64 (2011), pp. 966–969.
[26] S.V. Ketov, Y.H. Sun, S. Nachum, Z. Lu, A. Checchi, A.R. Beraldin, H.Y. Bai, W.H. Wang, D.V. Louzguine-Luzgin, M.A. Carpenter, and A.L. Greer, *Rejuvenation of metallic glasses by non-affine thermal strain*, Nature 524 (2015), pp. 200–203.
[27] T.C. Hufnagel, *Cryogenic rejuvenation*, Nature Mater. 14 (2015), pp. 867–868.
[28] F.O. Méar, B. Lenk, Y. Zhang, and A.L. Greer, *Structural relaxation in a heavily cold-worked metallic glass*, Scripta Mater. 59 (2008), pp. 1243–1246.

[29] M.B. Bever, D.L. Holt, and A.L. Titchener, *The stored energy of cold work*, Prog. Mater. Sci. 17 (1972), pp. 5–177.
[30] Y.H. Sun, A. Concustell, and A.L. Greer, *Thermomechanical processing of metallic glasses: extending the range of the glassy state*. Nature Rev. Mater. accepted for publication.
[31] L. Battezzati, G. Riontino, M. Baricco, A. Lucci, and F. Marino, *A DSC study of structural relaxation in metallic glasses prepared with different quenching rates*, J. Non-Cryst. Solids 61–62 (1984), pp. 877–882.
[32] A. Concustell, F.O. Méar, S. Suriñach, M.D. Baró, and A.L. Greer, *Structural relaxation and rejuvenation in a metallic glass induced by shot-peening*, Philos. Mag. Lett. 89 (2009), pp. 831–840.
[33] S.C. Glade, R. Busch, D.S. Lee, W.L. Johnson, R.K. Wunderlich, and H.J. Fecht, *Thermodynamics of $Cu_{47}Ti_{34}Zr_{11}Ni_8$, $Zr_{52.5}Cu_{17.9}Ni_{14.6}Al_{10}Ti_5$ and $Zr_{57}Cu_{15.4}Ni_{12.6}Al_{10}Nb_5$ bulk metallic glass forming alloys*, J. Appl. Phys. 87 (2000), pp. 7242–7248.
[34] I. Gallino, J. Schroers, and R. Busch, *Kinetic and thermodynamic studies of the fragility of bulk metallic glass forming liquids*, J. Appl. Phys. 108 (2010), Article ID 063501.
[35] L. Zhong, J. Wang, H. Sheng, Z. Zhang, and S.X. Mao, *Formation of monatomic metallic glasses through ultrafast liquid quenching*, Nature 512 (2014), pp. 177–180.
[36] M.D. Ediger and P. Harrowell, *Perspective: Supercooled liquids and glasses*, J. Chem. Phys. 137 (2012), Article ID 080901.
[37] R. Bhowmick, R. Raghavan, K. Chattopadhyay, and U. Ramamurty, *Plastic flow softening in a bulk metallic glass*, Acta Mater. 54 (2006), pp. 4221–4228.
[38] K.M. Flores, E. Sherer, A. Bharathula, H. Chen, and Y.C. Jean, *Sub-nanometer open volume regions in a bulk metallic glass investigated by positron annihilation*, Acta Mater. 55 (2007), pp. 3403–3411.
[39] S.G. Zaichenko, N.S. Perov, A.M. Glezer, E.A. Gan'shina, V.A. Kachalov, M. Calvo-Dalborg, and U. Dalborg, *Low-temperature irreversible structural relaxation of amorphous metallic alloys*, J. Magn. Magn. Mater. 215–216 (2000), pp. 297–299.
[40] S.G. Zaichenko and A.M. Glezer, *Physical model of the low-temperature-induced change in the structure and properties of amorphous alloys*, Doklady Phys. 47 (2002), pp. 846–848.
[41] K. Bán, A. Lovas, L. Novák, and K. Csach, *The influence of low temperature treatments on the H solubility and the Curie temperature of Fe-B based glasses*, Czech. J. Phys. 54 (2004), pp. D137–D140.
[42] K. Bán, A. Lovas, and J. Kováč, *Cryogenic effects in the amorphous Curie temperature shift of Fe-based glassy alloys*, Czech. J. Phys. 54 (2004), pp. D141–D144.
[43] H.S. Chen and E. Coleman, *Structure relaxation spectrum of metallic glasses*, Appl. Phys. Lett. 28 (1976), pp. 245–247.
[44] H.E. Kissinger, *Reaction kinetics in differential thermal analysis*, Anal. Chem. 29 (1957), pp. 1702–1706.
[45] H.B. Yu, W.H. Wang, and K. Samwer, *The β relaxation in metallic glasses: An overview*, Mater. Today 16 (2013), pp. 183–191.
[46] G.P. Johari and M. Goldstein, *Viscous liquids and the glass transition. II. Secondary relaxations in glasses of rigid molecules*, J. Chem. Phys. 53 (1970), pp. 2372–2388.
[47] H.B. Yu, X. Shen, Z. Wang, L. Gu, W.H. Wang, and H.Y. Bai, *Tensile plasticity in metallic glasses with pronounced β relaxations*, Phys. Rev. Lett. 108 (2012), Article ID 015504.
[48] X.D. Wang, Q.P. Cao, J.Z. Jiang, H. Franz, J. Schroers, R.Z. Valiev, Y. Ivanisenko, H. Gleiter, and H.-J. Fecht, *Atomic-level structural modifications induced by severe plastic shear deformation in bulk metallic glasses*, Scripta Mater. 64 (2011), pp. 81–84.
[49] S. Butler and P. Harrowell, *The shear induced disordering transition in a colloidal crystal: Nonequilibrium Brownian dynamic simulations*, J. Chem. Phys. 103 (1995), pp. 4653–4671.
[50] H. Löwen, *Colloidal soft matter under external control*, J. Phys. Condens. Matter 13 (2001), pp. R415–R432.
[51] C.-M. Lee, K.-W. Park, B.-J. Lee, Y. Shibutani, and J.-C. Lee, *Structural disordering of amorphous alloys: A molecular dynamics analysis*, Scripta Mater. 61 (2009), pp. 911–914.
[52] W. Thomson, *On the thermo-elastic and thermo-magnetic properties of matter*, Quart. J. Pure Appl. Math. 1 (1857), pp. 57–74.

[53] W. Thomson, *On the thermoelastic, thermomagnetic, and pyroelectric properties of matter*. Philos. Mag. Ser. 5, 5:28 (1878), pp. 4–27. doi:10.1080/14786447808639378
[54] X. Moya, S. Kar-Narayan, and N.D. Mathur, *Caloric materials near ferroic phase transitions*, Nature Mater. 13 (2014), pp. 439–450.
[55] T.C. Hufnagel, R.T. Ott, and J. Almer, *Structural aspects of elastic deformation of a metallic glass*, Phys. Rev. B 73 (2006), Article ID 064204.
[56] T. Egami, T. Iwashita, and W. Dmowski, *Mechanical properties of metallic glasses*, Metals 3 (2013), pp. 77–113.
[57] Y. Luo, Q.-K. Li, and M. Li, *Mechanical anisotropy at the nanoscale in amorphous solids*, J. Appl. Phys. 117 (2015), Article ID 044301.
[58] T. Egami and D. Srolovitz, *Local structural fluctuations in amorphous and liquid metals: a simple theory of the glass transition*, J. Phys. F: Met. Phys. 12 (1982), pp. 2141–2163.
[59] F. Albano and M.L. Falk, *Shear softening and structure in a simulated three-dimensional binary glass*, J. Chem. Phys. 122 (2005), Article ID 154508.
[60] J.C. Ye, J. Lu, C.T. Liu, Q. Wang, and Y. Yang, *Atomistic free-volume zones and inelastic deformation of metallic glasses*, Nature Mater. 9 (2010), pp. 619–623.
[61] D. Weaire, M.F. Ashby, J. Logan, and M.J. Weins, *On the use of pair potentials to calculate the properties of amorphous metals*, Acta Metall. 19 (1971), pp. 779–788.
[62] A.H. Taghvaei, H. Shakur Shahabi, J. Bednarčik, and J. Eckert, *Inhomogeneous thermal expansion of metallic glasses in atomic-scale studied by in situ synchrotron X-ray diffraction*, J. Appl. Phys. 117 (2015), Article ID 044902.
[63] E. Grüneisen, *Theorie des festen Zustandes ein-atomiger Element*, Ann. Physik 39 (1912), pp. 257–306.
[64] M.D. Ediger, *Spatially heterogeneous dynamics in supercooled liquids*, Annu. Rev. Phys. Chem. 51 (2000), pp. 99–128.
[65] A.S. Argon, *Plastic deformation in metallic glasses*, Acta Metall. 27 (1979), pp. 47–58.
[66] J. Pan, Q. Chen, L. Liu, and Y. Li, *Softening and dilatation in a single shear band*, Acta Mater. 59 (2011), pp. 5146–5158.

Appendix 1

We collect here some data and estimates used in calculating the parameter values given in the main text (especially Table 1).

Table A1:

Glass composition (at. %)	Gramme-atomic quantities: Mass (g)	Gramme-atomic quantities: Volume (cm^3)	Ref.
$Cu_{50}Zr_{50}$	77.38		(i)
		10.46	[A1]
$Cu_{57}Zr_{43}$	75.45		(i)
		9.96	(ii)
$Cu_{65}Zr_{35}$	73.23		(i)
		9.39	(ii)
$La_{55}Ni_{20}Al_{25}$	94.88		(i)
		15.90	(iii)
$Ni_{62}Nb_{38}$	71.71		(i)
		8.53	[A1]

(i) Calculated from standard atomic weights.
(ii) Estimated by interpolation between the values for $Cu_{50}Zr_{50}$ [A1] and for $Cu_{66}Zr_{34}$ (9.32 cm^3 $g\text{-}atom^{-1}$) [A2].
(iii) We use the value determined for $La_{55}Cu_{10}Ni_5Co_5Al_{25}$ [A1].
(iv) We use the value determined for $Ni_{60}Nb_{35}Sn_5$ [A1].

Thermal cycling of $La_{55}Ni_{20}Al_{25}$

Noting that the linear CTE of metallic glasses is ~12% higher than that of the counterpart crystalline state [A3], and taking the latter as the weighted (at.%) average of the CTE values of the constituent crystalline elements, we roughly estimate the linear CTE of the $La_{55}Ni_{20}Al_{25}$ melt-spun glass to be 1.3×10^{-5} K^{-1}.

We take the specific heat capacity of $La_{55}Ni_{20}Al_{25}$ melt-spun glass to be at the Dulong–Petit limit of 25 J K^{-1} g-atom^{-1}. The Kopp–Neumann law gives the specific heat per unit mass of a compound as the average, by mass fraction, of the specific heat per unit mass of the constituent elements. Applying this law for $La_{55}Ni_{20}Al_{25}$, and taking literature values for the element specific heats at room temperature, gives the similar value of 26.49 J K^{-1} g-atom^{-1}.

References

[A1] W.H. Wang, *The elastic properties, elastic models and elastic perspectives of metallic glasses*, Prog. Mater. Sci. 57 (2012), pp. 487–656.

[A2] Y. Calvayrac, A. Quivy, J.-P. Chevalier, and J. Bigot, *Effect of ternary additions on Cu-Zr glasses around the composition $Cu_{60}Zr_{40}$: still an ideal solid solution?* in *Rapidly Quenched Metals*, S. Steeb and H. Warlimont, eds., Elsevier, Amsterdam, 1985, pp. 455–458.

[A3] T. Komatsu, K. Matusita and R. Yokota, *Compositional dependence of thermal expansion coefficient of metallic glasses*, J. Non-Cryst. Sol. 72 (1985), pp. 279–286.